Journal of Biomedical Optics

SPIEDigitalLibrary.org/jbo

Microscopic structural study of collagen aging in isolated fibrils using polarized second harmonic generation

Dora Aït-Belkacem
Marie Guilbert
Muriel Roche
Julien Duboisset
Patrick Ferrand
Ganesh Sockalingum
Pierre Jeannesson
Sophie Brasselet

SPIE

Microscopic structural study of collagen aging in isolated fibrils using polarized second harmonic generation

Dora Aït-Belkacem,[a*] Marie Guilbert,[b*] Muriel Roche,[a] Julien Duboisset,[a] Patrick Ferrand,[a] Ganesh Sockalingum,[b] Pierre Jeannesson,[b] and Sophie Brasselet[a]
[a]Aix-Marseille Université, Institut Fresnel, CNRS UMR 7249, Ecole Centrale, Marseille, Domaine Universitaire St. Jérôme, 13013 Marseille, France
[b]Université de Reims Champagne-Ardenne, MéDIAN, FRE CNRS/URCA 3481, UFR de Pharmacie, 51 rue Cognacq-Jay, 51096 Reims, France

Abstract. Polarization resolved second harmonic generation (PSHG) is developed to study, at the microscopic scale, the impact of aging on the structure of type I collagen fibrils in two-dimensional coatings. A ribose-glycated collagen is also used to mimic tissue glycation usually described as an indicator of aging. PSHG images are analyzed using a generic approach of the molecular disorder information in collagen fibrils, revealing significant changes upon aging, with a direct correlation between molecular disorder and fibril diameters. [DOI: 10.1117/1.JBO.17.8.080506]

Keywords: aging; collagen fibrils; microscopy; molecular order; polarization; second-harmonic generation.

Paper 12249L received Apr. 21, 2012; revised manuscript received Jun. 19, 2012; accepted for publication Jun. 19, 2012; published online Aug. 14, 2012.

1 Introduction

Understanding the process of tissue aging is the center of a large research interest which has been strongly focused on investigations on collagen, the most abundant long-life structural protein in humans. It has been demonstrated that during normal aging, type I collagen loses flexibility, becomes stiffer, less soluble and more resistant to enzyme digestion.[1] These age-related changes have a direct impact on tissue organization and its biomechanical properties, leading to tissue damages.[2] They are mainly due to post-translational modifications such as tissue glycation,[3] leading to the formation of the so-called advanced glycation end products (AGEs) implicated in numerous physiopathological complications.[4] Nonlinear optical microscopy techniques have been recently introduced to study skin aging using two-photon excited autofluorescence (TPEF) (essentially from AGEs and elastin) and second harmonic generation (SHG) (from collagen). These studies focus essentially on the morphological alterations of the collagen network,[5,6] or on scoring indicators (such as the TPEF/SHG intensity ratio) as markers of collagen degradation.[7,8] While these analyses are performed at a macroscopic scale, the knowledge of microscopic scale molecular processes is still necessary to better understand the impact of aging on the collagen biomechanical properties.

In this work, we investigate the microscopic scale structural behavior of different-age type I collagen isolated fibrils using polarization resolved SHG (PSHG). This technique has been used in tissues;[9–11] however, recent works have underlined the complexity of its application in such complex samples, where scattering and birefringence can lead to polarization distortions.[12,13] To avoid such complication, we focus our study on a two-dimensional (2-D) model system made of coated type I collagen isolated fibrils submicrometric thickness.[14] To analyze PSHG data, a symmetry decomposition of the molecular orientational distribution in collagen fibrils is implemented, which permits to access to local molecular order information in a generic approach without invoking an *a priori* model for the molecular orientation, as usually done.[9–11]

2 Materials and Methods

Acid-extracted, native type I collagens were isolated from newborn (four to six days), young adult (two months), six months), and old (two years) rat tail tendons. For each age-group, the number of sacrificed animals had to be adjusted in order to reach the same yield of collagen (1 g): 105 (newborn), 8 (young adult), 7 (adult), and 5 (old). Glycated collagen was obtained by incubating at 4°C for five days the lyophilized collagen (1 mg/ml) with 3 M of ribose in 0.15 M phosphate buffer pH 7.4. Then collagens were extensively dialyzed against distilled water and lyophilized.[15] For 2-D coatings, lyophilized collagens solubilized in 18 mM acetic acid were coated on the surface of a 4-well chambered coverglass Lab-TeK system (Nunc, France), at a concentration of 150 $\mu g/cm^2$. Then coated substrates were dried overnight at room temperature and rinsed in water.[14]

The PSHG imaging set-up is based on an inverted two-photon excitation microscope in which the incident wavelength 800 nm from a Ti:Sapphire laser is focused by a high numerical aperture objective (NA 1.15) after reflection on a dichroic mirror. Images are performed by scanning the beam in the sample plane using galvanometric mirrors at a rate of about 1 image per second. The detected SHG signal is filtered at 400 nm and directed toward a photomultiplier. We ascertained that the sample does not affect the incident polarization by scattering or birefringence;[12] therefore, an unpolarized detection can be used. Polarization distortions from the optical set-up were also characterized beforehand and included in the signal analysis.[12] PSHG consists in rotating the incident linear polarization using a half wave plate on a step motor mount, recording one image per incident polarization between $\alpha = 0$- deg (relative to the horizontal direction in the sample plane) and 180-deg in 32 steps.

The data analysis uses a Fourier decomposition of the polarization dependence signal $I^{SHG}(\alpha) = a_0 + a_2\cos(2\alpha) + b_2\sin(2\alpha) + a_4\cos(4\alpha) + b_4\sin(4\alpha)$,[11] from which molecular order information is deduced following a methodology described previously.[16] In this generic approach, nonlinear active molecules of collagen fibrils are considered to lie within a molecular distribution function which can be reduced to a 2-D function:[16]
$f(\phi) = p_1\cos(\phi-\phi_0) + p_3\cos(3(\phi-\phi_0)) + q_3\sin(3(\phi-\phi_0))$,

*These authors contributed equally to this work.

Address all correspondence to: Sophie Brasselet, Aix-Marseille Université, Institut Fresnel, CNRS UMR 7249, Ecole Centrale, Marseille, Domaine Universitaire St Jérôme, 13013 Marseille, France. Tel: 04-91 28 84 94; Fax: 04-91 28 80 67; E-mail: sophie.brasselet@fresnel.fr

0091-3286/2012/$25.00 © 2012 SPIE

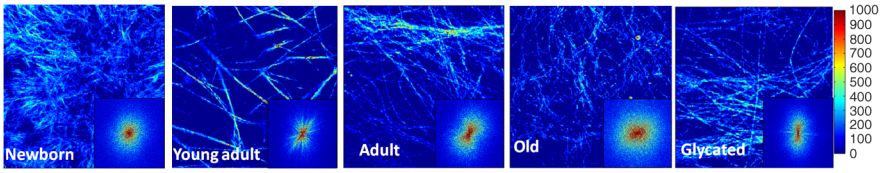

Fig. 1 SHG intensity images of coated type I collagen fibrils (and corresponding 2-D FFT maps shown as insets), as a function of age and for ribose-glycation. Vertical scale: total photon counts summed over 32 incident polarization angles. Image size: 90×90 μm^2 (300×300 pixels). Averaged incident power: 10 mW at the sample plane.

with ϕ the angle between the individual molecule's axis and the horizontal direction X in the sample plane, and ϕ_0 the global orientation of the distribution with respect to X. The so-called order parameters (p_1, p_3, q_3) are deduced from the normalized Fourier coefficients $(a_2/a_0, \cdots, b_4/a_0)$ by minimizing the mean square error between experimental coefficients and theoretical predictions.[16] The quantity $p = p_3/p_1$ is used as an indicator of molecular order, while q_3 indicates an asymmetry of the distribution.[16] This model is general and does not require an *a priori* known molecular distribution to quantify molecular order. For the comparison of different age conditions, 20 subregions of the SHG images in each age-group (50×50 pixels size), where the fibrils are the most isolated, were considered. The quantities "SHG efficiencies" and "p values" considered for ANOVA statistical analyses ($n = 20$) were averaged over each subregion and represented by their mean and standard error of the mean (SEM).

3 Results and Discussion

SHG intensity images of four different-age coated type I collagens (newborn, young adult, adult, and old) and ribose-glycated collagen are presented in Fig. 1. A direct morpho logical observation of these collagens, coated at the same concentration, show fibril networks and individual fibrils that become thicker and sparser in young adults compared to newborns. In addition, their length markedly increases with the age of the specimens. Two-dimensional fast Fourier transform (FFT) representations of the corresponding images (Fig. 1) show furthermore that a 1D straight structure of fibrils is highly pronounced for young adults (with visible privileged orientations in the FFT image), less pronounced for adults, and absent in the cases of newborn and old rats. As a comparison, the glycated sample is close to the adult case (Fig. 1). The averaged diameter of the fibrils [Fig. 2(a)], which is above the 300 nm diffraction limit size, shows a similar trend with thicker fibrils for the young adults. Although the glycated sample exhibits a similar morphology as the adults, it is constituted of thicker fibrils. The averaged SHG intensity of the images [Fig. 2(c)] seems to be correlated with the fibril diameters, the higher SHG intensity of thicker fibrils being most probably a signature of their higher collagen content.

For each age condition, the analysis of PSHG signals was performed on images taken in different regions of the whole sample surface. Only pixels exhibiting a total SHG signal above 150 photons are considered, which ensures that the measurements are not dominated by noise.[16] Typical retrieved images for the orientation (ϕ_0) and molecular order (p) parameters are shown in Fig. 3(a). q_3 is found to be close to 0 in all cases, indicating cylindrical-symmetry distributions along the fibrils.[16] The ϕ_0 angle is well correlated with the macroscopic fibril orientation. The p-image shows a large distribution of values, most probably due to intrinsic heterogeneities in fibril morphologies and to the diversity present within the rat's population of each age-group. However, in spite of such intra-age heterogeneities, inter-age variations are pronounced and can be clearly observed [Fig. 3(c), ANOVA on $n = 20$ subregions], with a significance probability below 5% except between adult and young adult cases. The maximum molecular order (high p values) is obtained for the newborn and old collagens. Since molecular order is representative of how fibrils are oriented with respect to each other, a large p value indicates a low degree of orientational freedom for molecules constituting the fibrils, also interpreted as a lower aperture of their angular distribution [Fig. 3(d)].[9–11,16] The large p value observed in the newborn group can therefore be attributed to higher structural constraint and rigidity, which is *a priori* contradictory with the higher elastic modulus observed in newborn collagen three-dimensional (3-D) matrices.[17] Elasticity can be however ascribed to a more macroscopic scale effect related to the length of fibrils, which appears to increase with age. Finally, young adult fibrils show a lower molecular order, signature of a more complex assembly of individual fibrils within their thicker fibers.

For the glycated collagen, data shown in Figs. 2 and 3 indicate that at a microscopic scale, *in vitro* glycation does not corroborate with an advanced-age situation, as it has been so far described in the literature.[8] Taken together, our data are in agreement with a recent SHG analysis of the collagen index orientation in mice dermal tissue which shows that younger skin

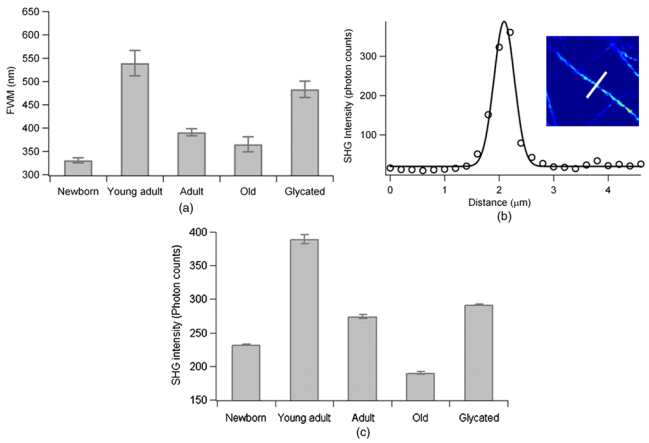

Fig. 2 (a) Fibril diameter at Full Width Half Maximum (FWHM) as a function of age of the collagen fibrils and for the ribose-glycated collagen ($n = 10$ fibrils were measured per condition, mean and SEM are shown). FWHM are obtained from a fit of Gaussian profiles from single fibrils. (b) Typical cross section of a young adult collagen fibril with Gaussian fit (continuous line, deduced FWHM 400 nm) on a fibril shown in the inset. The white bar corresponds to the profile support. (c) Average intensities (mean and SEM) measured over $n = 20$ subregions of the SHG images for each age-group (see text). All conditions were significantly different at 1% level (One way ANOVA, Tukey HSD test).

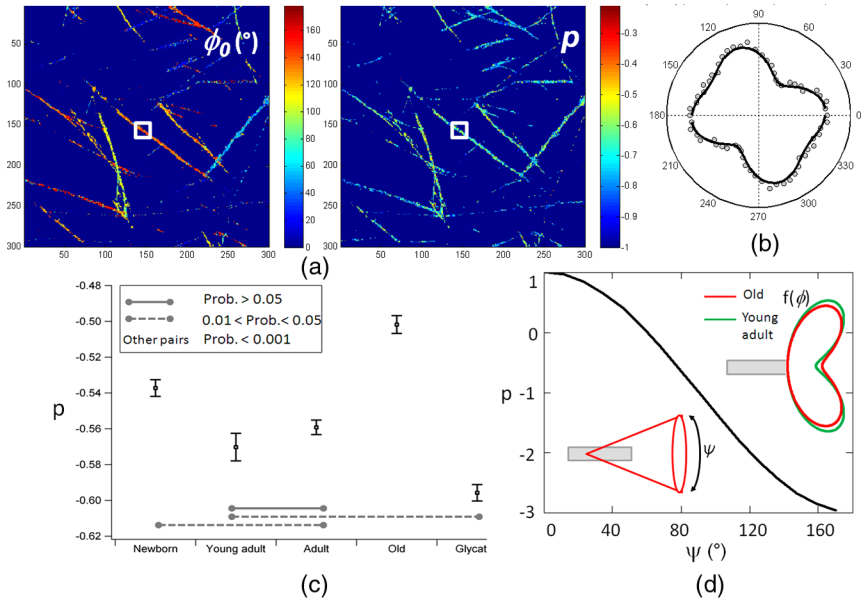

Fig. 3 (a) Images deduced from PSHG analysis in a young adult sample: averaged orientation (ϕ_0) of the fibrils relative to the horizontal axis obtained from the circular decomposition angle (see text) and retrieved molecular order (p) parameter. (b) Typical PSHG data, recorded in the area represented by the white square. (c) Comparison of the averaged p values (mean and SEM) for different age-groups and ribose-glycated collagen fibrils ($n = 20$ subregions of the SHG images). The lines indicate significant differences in mean values between conditions (One way ANOVA, Tukey HSD test). (d) Dependence of p relative to the angular cone aperture (Ψ) of molecules inside fibrils assemblies. Schematic representation of the molecular orientational distribution in the collagen fibril (represented by the grey cylinder), showing in polar plots the probability of orientation of individual molecules constituting a fibril along the cylinder axis.

exhibits a fine texture whereas aged skin displays a rougher texture.[6] In addition, they suggest that *in vitro* glycated collagen does not represent a good model for studying aged collagen at the microscopic scale.

4 Conclusion

We demonstrate the feasibility of a direct microscopic analysis of different-age type I collagen fibrils using PSHG microscopy. The observed differences between the microscopic structure of newborn and adult fibrils are not necessarily correlated with their macroscopic elasticity properties. This information can be potentially used in tissue samples, particularly in situations where early diagnosis based on subtle morphological changes is a challenge.

Acknowledgments

We thank Philippe Réfrégier for his contribution in the development of the theoretical model. This work is supported by CNRS, the Région Provence Alpes Côte d'Azur and the Région Champagne-Ardenne.

References

1. N. C. Avery and A. J. Bailey, "The effects of the Maillard reaction on the physical properties and cell interactions of collagen," *Pathol. Biol.* **54**(7), 387–395 (2006).
2. K. Mikuliková et al., "Study of postranslational non-enzymatic modifications of collagen using capillary electrophoresis/mass spectroscopy and high performance liquid chromatography/mass spectroscopy," *J. Chromatogr. A* **1155**(2), 125–133 (2007).
3. R. G. Paul and A. J. Bailey, "Glycation of collagen: the basis of its central role in the late complications of ageing and diabetes," *Int. J. Biochem. Cell Biol.* **28**(10), 1297–1310 (1996).
4. G. Kesava Reddy, "Cross-linking in collagen by nonenzymatic glycation increases the matrix stiffness in rabbit achilles tendon," *Exp. Diab. Res.* **5**(2), 143–153 (2004).
5. M. Johannes Koehler et al., "Morphological skin ageing criteria by multiphoton laser scanning tomography: non-invasive in vivo scoring of the dermal fibre network," *Exp. Dermatol.* **17**(6), 519–523 (2008).
6. S. Wu et al., "Quantitative analysis on collagen morphology in aging skin based on multiphoton microscopy," *J. Biomed. Opt.* **16**(4), 040502 (2011).
7. M. J. Koehler et al., "In vivo assessment of human skin aging by multiphoton laser scanning tomography," *Opt. Lett.* **31**(19), 2879–2881 (2006).
8. J-Y. Tseng et al., "Multiphoton spectral microscopy for imaging and quantification of tissue glycation," *Biomed. Opt. Express* **2**(2), 218–230 (2011).
9. P. Stoller et al., "Polarization-modulated second harmonic generation in collagen," *Biophys. J.* **82**(6), 3330–3342 (2002).
10. R. M. Williams, W. R. Zipfel, and W. W. Webb," Interpreting second-harmonic generation images of collagen I fibrils," *Biophys. J.* **88**(2), 1377–1386 (2005).
11. S. Psilodimitrakopoulos et al., "In vivo, pixel-resolution mapping of thick filaments' orientation in nonfibrilar muscle using polarization-sensitive second harmonic generation microscopy," *J. Biomed. Opt.* **14**(1), 014001 (2009).
12. D. Aït-Belkacem et al., "Influence of birefringence on polarization resolved nonlinear microscopy and collagen SHG structural imaging," *Opt. Express* **18**(14), 14859–14870 (2010).
13. I. Gusachenko, G. Latour, and M.-C. Schanne-Klein, "Polarization-resolved second harmonic microscopy in anisotropic thick tissues," *Opt. Express* **18**(18), 19339–19352 (2010).
14. N. Fourre et al., "Extracellular matrix proteins protect human HT1080 cells against the antimigratory effect of doxorubicin," *Cancer Sci.* **99**(8), 1699–1705 (2008).
15. G. Said et al., "Impact of carbamylation and glycation of collagen type I on migration of HT1080 human fibrosarcoma cells," *Int. J. Oncol.* **40**(6), 1797–1804 (2012).
16. J. Duboisset et al., "Generic model of the molecular orientational distribution probed by polarization resolved second harmonic generation," *Phys. Rev. A* **85**, 043829 (2012).
17. S. L. Wilson et al., "The effect of collagen ageing on its structure and cellular behavior," *Proc. SPIE* **8222**, 822210 (2012).